

Thermal stability of exchange-coupled magnetic grains

F. C. S. da Silva* and J. P. Nibarger

Magnetic Technology Division, National Institute of Standards and Technology, Boulder, Colorado 80305, USA

(Received 12 February 2003; published 31 July 2003)

We analyzed the effects of exchange interactions on the thermal stability of magnetic grains in perpendicular recording media. We modeled the magnetic properties of single-domain, uniformly oriented grains using the master equation formalism and the mean-field theory for systems with anisotropy. In the absence of applied fields and for exchange fields much smaller than the anisotropy field, the relaxation time of the system increases linearly with the exchange field amplitude. In the presence of applied fields, exchange interactions and thermal fluctuations improve the switching dynamics of the system leading to a reduction in the energy barrier distribution width and a reduction in the switching field amplitude. For both cases, we propose analytic expressions for the thermal dependence of the relaxation time and the switching field.

DOI: 10.1103/PhysRevB.68.012414

PACS number(s): 75.10.Hk, 75.50.Tt, 75.50.Ss, 85.70.Ay

The superparamagnetic limit of magnetic nanograins in recording media has been discussed thoroughly in recent years.^{1,2} The description of these systems is normally based on analytical models for interacting³ and noninteracting grains,⁴ and on micromagnetic simulations.^{5,6} For the particular case where exchange interactions are considered, experimental⁷ and numerical⁸ results show an improvement of thermal stability in the system. The main results for increasing exchange fields report a reduction of the width of the switching field distribution together with an increase in the coercivity, activation volume, and blocking temperature. Nevertheless, a simple analytic expression that relates the effect of exchange on the thermal stability of the grains is yet to be proposed.⁹ We present a method to analyze the effect of exchange interactions between grains in recording media. The method uses the mean-field theory for systems with anisotropy, which was developed initially to describe effects of exchange interactions on atomic systems with random anisotropy.¹⁰ Two cases are considered. In the first, we assume no applied field to calculate the mean effect of exchange interactions on the relaxation time of the system. In the second, we assume static fields, applied in sequence (as in a hysteresis loop) to compute the magnetic moment using the master equation (ME) formalism. For both cases, analytic expressions for the thermal dependence of the relaxation time and switching field are obtained.

We use the Stoner-Wohlfarth model to describe the behavior of individual magnetic grains under the influence of the mean exchange field. The exchange field is a consequence of the exchange interaction mediated by the grain boundaries or by a soft underlayer. We assume that each grain can be considered as a single domain and that neighboring grains can interact via exchange only. The system is considered to be uniaxial, with the magnetic energy given by

$$E = -MVH_{eff}\cos\theta - KV\cos^2(\phi - \theta), \quad (1)$$

where M , V , and K are the saturation magnetization, the volume, and the magnetocrystalline uniaxial anisotropy constant of each grain, respectively. The angles ϕ and θ are those

formed by the anisotropy axis and the magnetic-moment vector of the grain relative to the effective field H_{eff} , given by

$$H_{eff} = H_{app} + mH_{ex}, \quad (2)$$

where H_{app} is the applied field and H_{ex} is the mean exchange field amplitude. H_{ex} is proportional to the exchange constant J and the number of nearest neighbors of each grain.¹⁰ H_{ex} is modulated by m , which is the average projection of the equilibrium moment vectors along the applied field direction \hat{z} . Since the easy axes are distributed on the hemisphere according to some distribution function $g(\phi)$, quantity m is given by

$$m = \langle \cos\theta \rangle_{\phi} = \frac{\int_0^{\pi/2} \cos[\theta(\phi)]g(\phi)\sin(\phi)d\phi}{\int_0^{\pi/2} g(\phi)\sin(\phi)d\phi}. \quad (3)$$

The solution for $g(\phi) = 1$ has been obtained for $T = 0$ K (Ref. 10) and for $T \neq 0$ K (Ref. 13) by solving Eqs. (2) and (3) simultaneously and assuming that the exchange field is in the \hat{z} direction. This assumption is coherent with the fact that there is no preferred orientation since the anisotropy axes are distributed uniformly. In these cases, exchange interactions reduce the overall coercivity of the system by averaging out the local anisotropy.

Here, we focus on a different case, where $g(\phi) = \delta(\phi)$, i.e., all the grains are oriented along the applied field axis. In this case, Eq. (3) gives $m = \cos\theta$, and a direct substitution of Eq. (2) into Eq. (1) leads to an additional term in the anisotropy constant that is proportional to H_{ex} . The anisotropy field amplitude of the interacting system is then given by

$$H_{an} = H_{an}^o(1 + 2h_{ex}), \quad (4)$$

where $H_{an}^o \equiv 2K/M$ is the anisotropy field for each grain and $h_{ex} \equiv H_{ex}/H_{an}^o$ is the normalized exchange field. The energy barrier of the system at zero applied field also increases lin-

early with h_{ex} . Therefore the relaxation time τ in the Arrhenius-Néel formula has now an exchange term

$$\tau = \tau_o \exp \left[\frac{KV(1+2h_{ex})}{k_B T} \right], \quad (5)$$

where τ_o is a constant, k_B is Boltzmann's constant, and T is the temperature.

This result relates the effect of exchange on the increase of the effective activation volume observed experimentally in high-density perpendicular media.⁷ Equation (5) also confirms the expression obtained by Glauber¹¹ for a system of Ising spins with nearest-neighbor exchange interactions. In his paper, Glauber found that the relaxation dynamics is slowed by the presence of exchange interactions. In particular, for $h_{ex} \ll 1$, the relaxation time in Eq. (5) increases linearly with h_{ex} , which matches Glauber's prediction for small h_{ex} .

The thermal stability improvement due to h_{ex} does not mean that the coercivity of the system will also increase. In fact, the correlations provided by the exchange interactions also enhance the switching dynamics close to the switching field. This mechanism can be understood by considering small deviations of the easy axis orientation of each particle with respect to the applied field axis. This misalignment will naturally move the switching point of each particle out of the astroid's cusp and reduce the switching field along the applied field direction.¹² Since the exchange interactions are proportional to the relative angle between the nearest moments, the mean exchange field due to the misalignment between particles will also have a transverse field component. This component will be added to the transverse component of the applied field to reduce the longitudinal switching field.

For the case of perfectly aligned particles, the improvement in the switching dynamics is caused by thermal fluctuations (spin flips). Every thermally induced flip that happens at fields smaller than the switching field will add an extra negative field to the applied field. It is natural that the flipping probability decreases with exchange as shown by Eq. (5), but once a thermally induced flip happens, it drives the system faster to the new equilibrium state.

To calculate the effects of temperature and exchange interactions on the switching dynamics, we use the mean-field approach developed by Callen, Liu, and Cullen.¹⁰ We now define the *thermal* average of the magnetic moment for non-interacting particles

$$m = \langle \cos \theta \rangle_T, \quad (6)$$

and calculate the mean-field interactions by solving Eqs. (2) and (6) simultaneously. An analytical solution can be obtained graphically for $g(\phi) = \delta(\phi)$, as shown in Fig. 1(a). We assume that Eq. (6) provides a perfectly square demagnetizing branch of the hysteresis loop with the magnetization switching at $h_{eff} \equiv H_{eff}/H_{an}^o = -1$. Equation (2) can be solved for m , which describes a straight line of slope $1/h_{ex}$ intercepting the h_{eff} axis at the applied field $h_{app} \equiv H_{app}/H_{an}^o$.

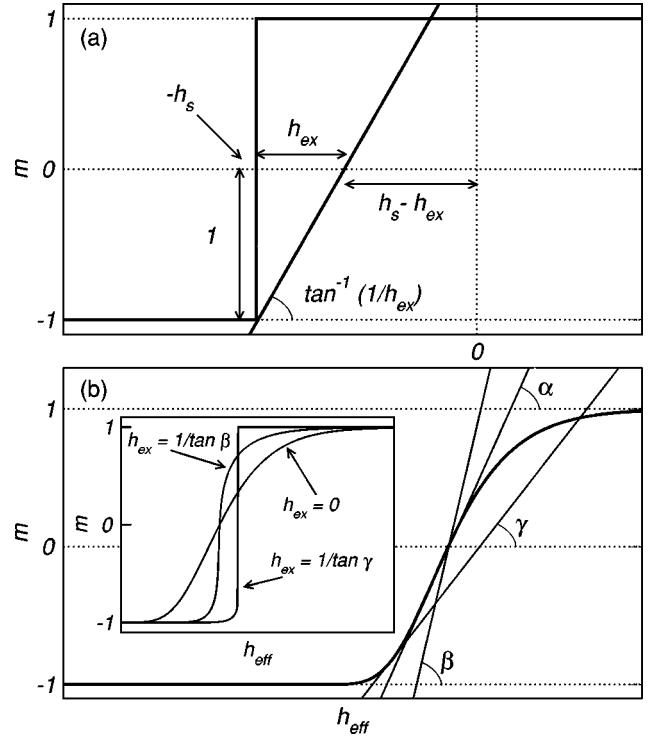


FIG. 1. Graphical solution of Eqs. (2) and (6). (a) The straight line is given by Eq. (2) solved for m . Equation (6) is approximated here to a perfectly square demagnetizing branch. (b) Equation (6) described by the ME formalism, with the highest slope given by α . The lines corresponding to β and γ relate to different values of the normalized exchange field $h_{ex} = H_{ex}/H_{an}^o$. The inset shows the solution of Eqs. (2) and (6) for different h_{ex} values.

Depending on the value of h_{app} , the line can intercept the demagnetizing branch at one or more points. We are interested in the case when h_{app} decreases to $-(h_s - h_{ex})$, as shown in Fig. 1(a). At this point, there are two possible solutions for m , but only $m = -1$ is stable since $h_{app} < 0$. Notice that the normalized switching field $h_s \equiv H_s/H_{an}^o$ decreases linearly with the exchange field amplitude, i.e., $h'_s = h_s - h_{ex}$.

In a more realistic description of Eq. (6), the demagnetizing curve is obtained by using a ME formalism.^{11,14} The ME describes the occupation f of the magnetic moments between the stable and metastable minimum states of the system. These two states are defined by Eq. (1) for each h_{app} . The rate at which f changes in time is then given by

$$\frac{df}{dt} = \frac{1}{\tau_o} \left[-f \exp \left(-\frac{\Delta E_1}{k_B T} \right) + (1-f) \exp \left(-\frac{\Delta E_2}{k_B T} \right) \right], \quad (7)$$

where ΔE_i is the energy barrier for each minimum. The integration of Eq. (7) for time-varying applied fields can be obtained via a series expansion for small h_{app} .¹⁵ For large h_{app} , f can be obtained by assuming that h_{app} varies step by step. With this assumption, Eq. (7) can now be integrated exactly, since h_{app} is constant during the integration (measurement) time τ_m , giving

$$f = f_o \exp\left(-\frac{\tau_m}{\tau_o} A\right) + \frac{B}{A} \left[1 - \exp\left(-\frac{\tau_m}{\tau_o} A\right)\right], \quad (8)$$

where f_o is the initial fraction (before the step in h_{app}) and

$$A = \left[\exp\left(\frac{\Delta E_1}{k_B T}\right) + \exp\left(\frac{\Delta E_2}{k_B T}\right) \right], \quad (9)$$

$$B = \exp\left(\frac{\Delta E_2}{k_B T}\right). \quad (10)$$

Equation (8) can be used iteratively to generate the magnetization curve. For the particular case where $\phi=0$, $m=2f-1$. Once again, one can use the graphical construction shown in Fig. 1(b) to obtain the solution of Eqs. (2) and (6). The main difference is that the demagnetizing branch of the hysteresis loop now has a finite maximum derivative angle α at the switching point. If the exchange field is sufficiently small, e.g., $h_{ex}=1/\tan\beta$ as shown in Fig. 1(b), the line given by Eq. (2) will intercept the demagnetizing curve at only one point for each h_{app} . The inset in Fig. 1(b) shows that, in this regime, the switching region narrows, but no change in the switching field is observed. Therefore the squareness of the demagnetizing curve is enhanced when compared to the noninteracting curve. In the limit where $h_{ex}\rightarrow 0$, the noninteracting demagnetizing curve is restored.

For $h_{ex} > 1/\tan\alpha$, e.g., $h_{ex}=1/\tan\gamma$ as shown in Fig. 1(b), the line can intercept the demagnetizing curve in more than one point. The switching field is then redefined as the point at which the line crosses the demagnetizing curve in more than one point. This situation not only improves the squareness, but also forces the switching field to decrease as shown in the inset of Fig. 1(b). This result is similar to the analytical one described in Fig. 1(a).

A simulation of the thermal dependence of the switching field for $0 \leq h_{ex} \leq 1$ was performed using the ME formalism and the mean-field approach with the following parameters: $M=400 \text{ kA m}^{-1}$ (400 emu cm^{-3}), $K=2 \times 10^5 \text{ J m}^{-3}$ ($2 \times 10^6 \text{ erg cm}^{-3}$), $V=1.14 \times 10^{-24} \text{ m}^3$ (a cylinder 9 nm in diameter and 18 nm thick),¹⁶ $\tau_o=10^{-9} \text{ s}$, $\tau_m=0.1 \text{ s}$, 1000 points in the demagnetizing curve with $\delta h_{app}=0.003$ and $-1.5 \leq h_{app} \leq 1.5$. These parameters provided the anisotropy field $H_{an}^o=800 \text{ kA m}^{-1}$ (10 kOe).

Figure 2(a) shows the thermal dependence of the normalized switching field for different values of h_{ex} . For $h_{ex}=0$, the curve reproduces the thermal dependence of the switching field for a set of noninteracting monodomain grains aligned along the applied field. For this case, the simulation provides an initial blocking temperature T_b^o of 798 K. The simulated curves of Fig. 2(a) were fitted using the equation

$$h_t \equiv \frac{H_t}{H_{an}^o} = h_t^o \left[1 - \left(\frac{T}{T_b^o} \right)^\eta \right]. \quad (11)$$

Simulations for other values of h_{ex} in the range $0 \leq h_{ex} \leq 1$ were also fitted using Eq. (11). The dependence of the

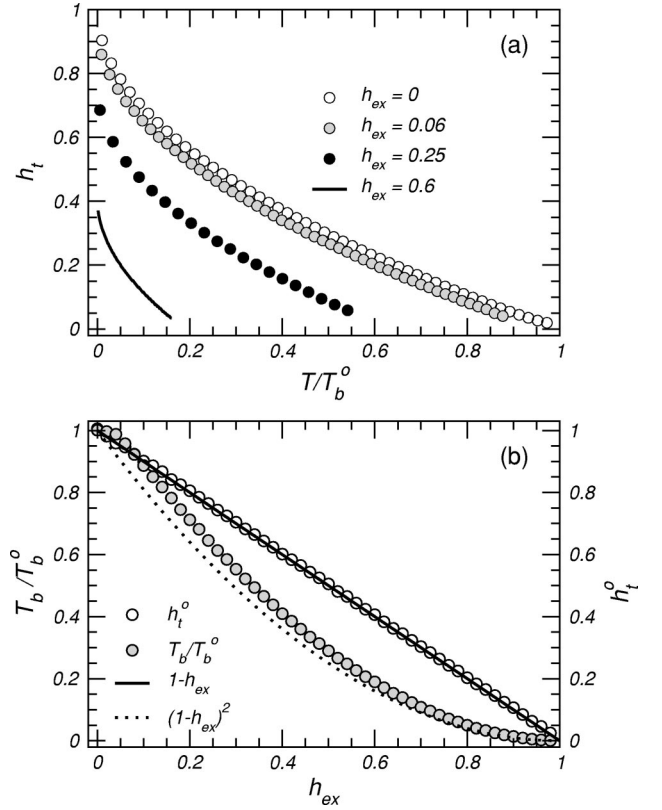


FIG. 2. (a) Thermal dependence of the normalized switching field h_t for different values of the normalized exchange field h_{ex} . (b) Dependence of the normalized blocking temperature T_b/T_b^o and the switching field amplitude h_t^o on the normalized exchange field h_{ex} given by Eq. (11).

fitting parameters h_t and T_b/T_b^o on h_{ex} is plotted in Fig. 2(b). Here, the solid and dotted lines represent the graphical solution obtained using Fig. 1(a). The exponent η was found to vary by 0.003 around a mean value of 0.509.

The results show that the exchange interactions, simulated using the ME formalism, are in good agreement with the predicted result of Fig. 1(a). This means that a square loop is an excellent first approximation for the magnetizing curve at $T \neq 0 \text{ K}$. The T_b/T_b^o curve deviates from the square loop prediction. This is due to thermally induced shearing of the demagnetizing branch that produces a finite maximum slope during the switching. From this result, we see that an external shearing component, e.g., out-of-plane anisotropies or demagnetizing fields, can be reduced by the presence of exchange interactions. Additionally, we have seen that the exchange interactions improve the squareness of the noninteracting loop. The simulations also show that exponent η is in agreement with the known prediction of $\eta=0.5$ (Ref. 4) for noninteracting grains aligned along the applied field.

The exchange interaction described in this model is a cooperative effect, i.e., it tends to align the magnetic moments along the same direction. This effect leads to two important consequences. First, it helps increase the energy barrier of the system, which improves the thermal stability. This helps explain the larger activation volume compared to the grain

size observed experimentally in perpendicular recording media. Second, exchange interactions enhance thermal fluctuation effects and destabilize the system more easily. This consequence has two implications on the recording media: a narrowing of the width of the switching field distribution and a reduction of the switching field amplitude. We have found

theoretically that these results lead to analytic expressions for the thermal dependence of the relaxation time and the switching field in terms of the normalized exchange field.

F.C.S.S. thanks Fundação de Amparo à Pesquisa do Estado de São Paulo for partial financial support.

*Electronic address: fcsc@boulder.nist.gov

¹S.H. Charap, P.L. Lu, and Y. He, *IEEE Trans. Magn.* **33**, 978 (1997).

²D. Weller and A. Moser, *IEEE Trans. Magn.* **35**, 4423 (1999).

³R.H. Victora, *Phys. Rev. Lett.* **63**, 457 (1989).

⁴M.P. Sharrock, *J. Appl. Phys.* **76**, 6413 (1994).

⁵O.A. Chubykalo, B. Lengsfeld, B. Jones, J. Kaufman, J.M. Gonzalez, R.W. Chantrell, and R. Smirnov-Rueda, *J. Magn. Mater.* **221**, 132 (2000).

⁶A. Lyberatos, *J. Phys. D* **33**, R117 (2000).

⁷Y. Sonobe, D. Weller, Y. Ikeda, K. Takano, M.E. Schabes, G. Zelter, H. Do, B.K. Yen, and M.E. Best, *J. Magn. Mater.* **235**, 424 (2001).

⁸H. Zhou, H.N. Bertram, A. F Torabi, and M.L. Mallery, *IEEE Trans. Magn.* **37**, 1558 (2001).

⁹H.N. Bertram, X. Wang, and V.L. Safanov, *IEEE Trans. Magn.* **37**, 1521 (2001).

¹⁰E. Callen, Y.J. Liu, and J.R. Cullen, *Phys. Rev. B* **16**, 263 (1977).

¹¹R.J. Glauber, *J. Math. Phys.* **4**, 294 (1963).

¹²E.C. Stoner and E.P. Wohlfarth, *Philos. Trans. R. Soc. London, Ser. A* **240**, 599 (1948).

¹³Y. Yu, S.T. Chui, and H.L. Shi, *Phys. Rev. B* **64**, 012401 (2001).

¹⁴I. Klik, C.R. Chang, and H.L. Huang, *Phys. Rev. B* **47**, 8605 (1993).

¹⁵I. Klik and Y.D. Yao, *J. Magn. Mater.* **186**, 233 (1998).

¹⁶See for example J.H. Judy, *J. Magn. Mater.* **235**, 235 (2001).